

Accurate Spectral Analysis of Two-Dimensional Point Sets

Thomas Schlömer and Oliver Deussen
University of Konstanz

Abstract. We investigate accuracy issues regarding the spectral analysis of two-dimensional point sets. We demonstrate the sensitivity of amplitude/power spectrum and radial statistics to the type of Fourier transform and formulate recommendations for crucial analysis and formatting parameters. The goal of these recommendations is to facilitate the comparison of different point-set generation methods with respect to their spectral characteristics.

1. Introduction

Spectral analysis is an important tool for evaluating two-dimensional point sets for computer graphics domains such as sampling, non-photorealistic rendering, or geometry processing. The Fourier amplitude spectrum, power spectrum estimate, radially averaged power spectrum, and anisotropy all help to reveal point-to-point correlations that could become problematic during their later application. For example, when sampling the image plane, the radial power spectrum of the sample points allows the identification of high energy peaks that could lead to coherent aliasing in the final image. Anisotropy, on the other hand, measures the radial symmetry of the spectrum, which helps to predict directional artifacts.

Figure 1 shows an exemplary spectral analysis of four classes of point sets obtained via stochastic and deterministic generation methods: (a) a Poisson reference distribution with a flat (white noise) power spectrum and

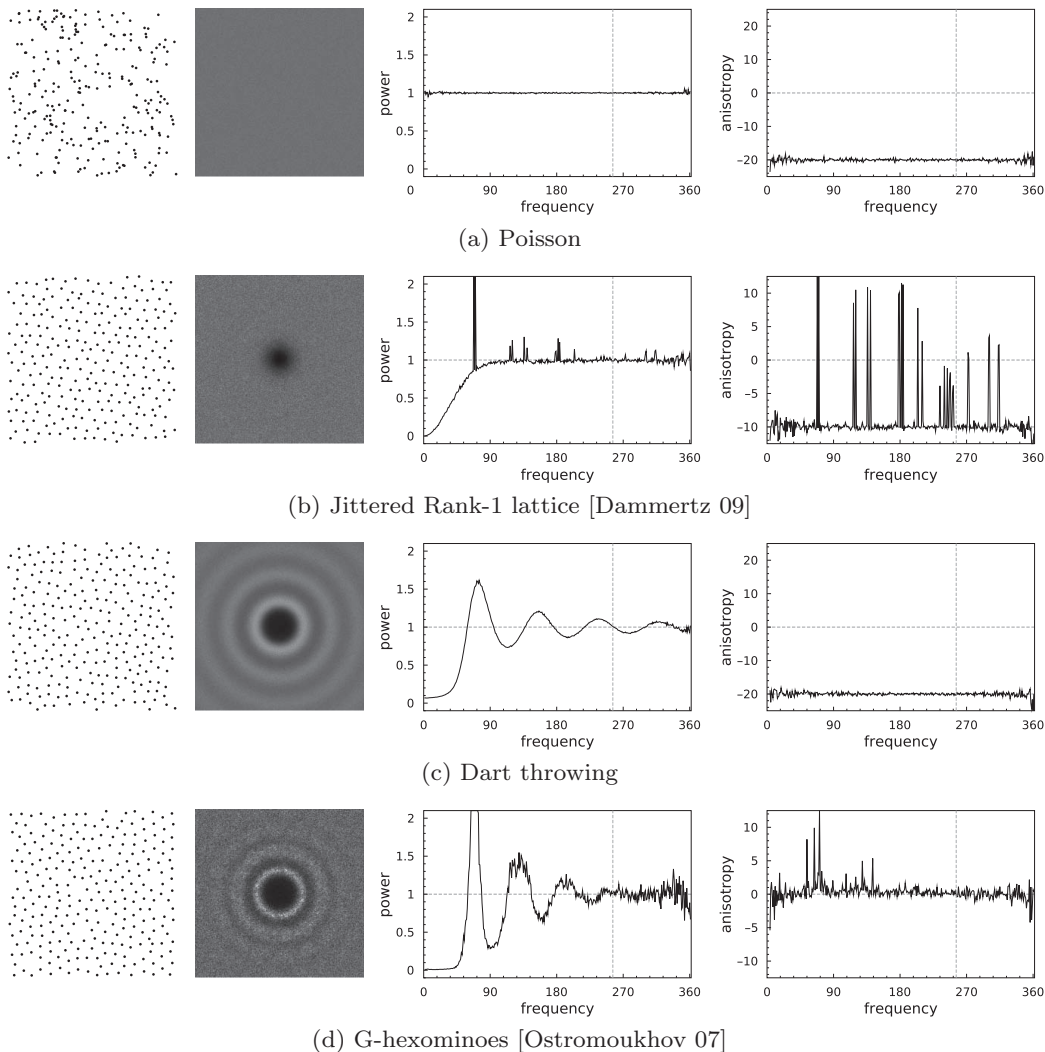


Figure 1. Spectral analysis of point sets obtained via (a)–(c) stochastic and (d) a deterministic generation method. Each figure shows (from left to right) an exemplary input point set, amplitude spectrum/power spectrum estimate, radially averaged power spectrum, and anisotropy.

no directional bias, (b) a jittered Rank-1 lattice with a circular region of low energy near the DC coefficient but peaks at several distinct frequencies in power spectrum and anisotropy, revealing the underlying lattice, (c) a stochastic Poisson-disk distribution obtained via dart throwing with a blue noise spectrum and flat anisotropy, and (d) a deterministic distribution obtained via a tile-based technique that aims for a similar blue noise frequency response but shows a slight directional bias.

As these evaluations are still largely qualitative, special care has to be taken with respect to the exact analysis and formatting parameters, the utilized

type of Fourier transform, and the applied mapping operators. Changing any of these variables may yield very different results, which prevents the unbiased comparison of different generation methods. In addition, the results described in this paper ensure maximum accuracy during the spectral analysis of point sets. It can be seen as a continuation of the established work by Ulichney [Ulichney 1987] and Lagae and Dutré [Lagae and Dutré 2008].

2. Background

We have to distinguish between deterministic and stochastic point generation methods. Deterministic methods always generate the same point set, whereas stochastic methods yield an ensemble of point sets. Deterministic point sets can be interpreted as finite energy signals that possess a Fourier transform. Hence, they are characterized by a corresponding Fourier amplitude spectrum. This does not apply to stochastic methods because of their inherent randomness. Instead, these methods can be regarded as stationary stochastic processes in which the main signal characteristic is complemented by noise [Proakis and Manolakis 96]. Such processes do not have finite energy but finite average power and, hence, are characterized by a corresponding power density spectrum.

2.1. Amplitude Spectrum

Let $Q = \{x_0, \dots, x_{n-1}\} \subset [0, 1)^2$ be a set of $n \geq 2$ two-dimensional points on the unit torus. Its Fourier transform \mathcal{F} can be determined by representing the point set as a superposition of Diracs $q(x) = \sum_{i=0}^{n-1} \delta(x - x_i)$. The normalized *amplitude spectrum* for deterministic point generation methods is then given by

$$A(\xi) = \frac{1}{n} |\mathcal{F}\{q(x)\}|,$$

where ξ denotes a real-valued spatial frequency $(\xi_x, \xi_y)^T$.

2.2. Power Spectrum Estimation

The power density spectrum $P(\xi)$ of a stationary stochastic process is the Fourier transform of its autocorrelation function (Wiener-Khinchin theorem). Since the autocorrelation function is seldom known, a spectral estimate of $P(\xi)$, $\overline{P}(\xi)$, must be obtained. Bartlett's method [Proakis and Manolakis 96]

of averaging K periodograms yields an unbiased and consistent estimator for the power spectrum, exhibits variance that decreases linearly with K , and is simple to implement.

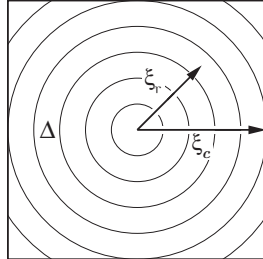
For real-valued signals, the *periodogram* is the squared magnitude of the Fourier transform. The *power spectrum estimate* $\overline{P}(\xi)$ is then given by the mean periodogram, which results from averaging K periodograms. Hence, the normalized power spectrum estimate for stochastic point generation methods is given by

$$\overline{P}(\xi) = \frac{1}{nK} \sum_{k=0}^{K-1} |\mathcal{F}\{q_k(x)\}|^2,$$

where the q_k represents unique point sets generated by the stochastic generation method. Its unit is W/Hz.

2.3. Radial Statistics

Ulichney [Ulichney 1987] derives two useful one-dimensional statistics from the power spectrum. The first is the *radially averaged power spectrum*



$$P_r(\xi_r) = \frac{1}{N_r(\xi_r)} \sum_{i=0}^{N_r(\xi_r)-1} \overline{P}(\xi_{r,i}), \quad (1)$$

which can be obtained by partitioning $\overline{P}(\xi)$ into concentric annuli of a fixed width Δ , and then averaging the $N_r(\xi_r)$ spectrum samples within each annulus of central radius ξ_r . The annuli start to exceed the spectral estimate at a critical frequency which we denote ξ_c .

The second statistic is the *anisotropy*

$$A_r(\xi_r) = \frac{V^2(\xi_r)}{P_r^2(\xi_r)}, \quad (2)$$

where $V^2(\xi_r)$ denotes the squared variance of the spectrum samples which is given by

$$V^2(\xi_r) = \frac{1}{N_r(\xi_r) - 1} \sum_{i=0}^{N_r(\xi_r) - 1} (\overline{P}(\xi_{r,i}) - P_r(\xi_r))^2.$$

Reference values for the radial power spectrum and the anisotropy can be obtained by considering a Poisson distribution of unit power which is depicted in Figure 1(a). Although both P_r and A_r are defined in terms of a power spectrum estimate, they can be equally applied to a given amplitude spectrum by replacing $\overline{P}(\xi)$ with $A(\xi)$ in Equations (1) and (2).

3. Accurate Spectral Analysis

The informative value and accuracy of these statistics depend on a number of analysis and formatting parameters, among them the type and frequency range of the Fourier transform, the number of periodograms, and the annulus width. In the following, we discuss each of the relevant parameters and show that the commonly used FFT is often not sufficient for accurate results.

3.1. Fourier Transform

For performance reasons, the Fourier transform (FT) of a point set Q is typically performed in its discrete variant as an FFT by translating Q into a discrete sample image. However, if we represent Q by $q(x) = \sum_{i=0}^{n-1} \delta(x - x_i)$ as discussed above, we can determine the (continuous) FT via

$$\begin{aligned} \mathcal{F}\{q(x)\} &= \mathcal{F}\left\{\sum_{i=0}^{n-1} \delta(x - x_i)\right\} \\ &= \sum_{i=0}^{n-1} \mathcal{F}\{\delta(x - x_i)\} \\ &= \sum_{i=0}^{n-1} e^{-2\pi i \xi x_i}, \end{aligned} \tag{3}$$

because \mathcal{F} is a linear operator. Thus, the frequency response for a given spatial frequency ξ can be determined analytically by a simple sum over all points x_i . This makes the calculation of the continuous FT not only computationally feasible but also more accurate than the commonly used FFT. Figure 2 demonstrates that this actually matters for accurate radial statistics where results based on an FFT significantly deviate from a CFT reference

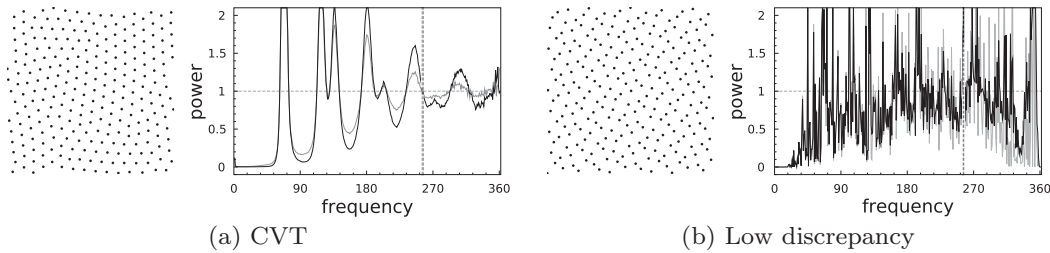


Figure 2. Radially averaged power spectrum based on a continuous FT (bold) and a discrete FT (light) for (a) the centroids of a centroidal Voronoi tessellation, and (b) a deterministic low-discrepancy point set.

solution. Although this effect can partly be remedied by a higher resolution FFT, it remains problematic for deterministic point sets whose Fourier transform is just a set of peaks (e.g., points that form a regular grid or Rank-1 lattices).

We also want to emphasize that the FT will be contaminated by boundary “artifacts” if the points are defined on the bounded unit square instead of the unit torus because the statistics of the generation process are then implicitly modified to exclude points outside the domain. For this reason, spectral analysis should be performed only on point sets that are periodic in space. This is already considered by most point-generation methods in graphics.

3.2. Frequency Range

For an accurate analysis, the amplitude spectrum and power spectrum estimates should span a range of frequencies that is broad enough to cover the characteristic frequency response of the specific generation method. Because the highest principal frequency can be achieved by a method that generates points with maximized mutual minimum distance, this implies at least a range of frequencies $[-N, N]$ with $N = w/d_{\max}$. Here, $d_{\max} = (2/(\sqrt{3}n))^{1/2}$ denotes the maximum minimum distance derived from the packing density of circles in the plane. The scalar $w \geq 1$ determines how much the spectrum window exceeds this frequency range in order to allow a proper view of the response. A suitable choice is $w = 4$ which is the value employed in this paper. We typically also round N to the next power of 2.

Using these conventions, the number of points n should be at least 1024, which yields the frequency range $[-128, 128]$. The figures in this paper were generated with $n = 4096$ and thus $N = 256$. In our experience, it is usually sufficient to sample the FT at the corresponding integer frequencies, which yields spectrum images of a resolution $2N \times 2N$.

3.3. *Number of Periodograms*

Using Bartlett’s method, the power spectrum estimate results from averaging K periodograms. Thus, a larger K yields smoother radial statistics than a smaller K (cf. Figures 1(c) and 1(d)). In our experience, $K \geq 10$ is required for a proper spectral analysis of stochastic generation methods but we recommend $K = 100$, as utilized in this paper.

Because we plot the anisotropy in decibels according to the relation $x_{\text{dB}} = 10 \log_{10} x$, a value of $-K$ dB implies background noise (cf. the Poisson reference distribution in Figure 1(a)). For this reason, anisotropy plots should contain a reference line at the appropriate noise level, for example, at 0, -10 , -20 for $K = 1, 10, 100$. Anisotropy close to the noise level indicates good radial symmetry for the specific generation method.

3.4. *Annulus Width*

The validity of the radial statistics obviously depends on the user-chosen annulus width Δ . In particular, Δ should not be too large because wide annuli effectively smooth the graphs and may hide subtle correlations in the analyzed point sets. In our experience, a width of approximately one frequency sample is sufficiently small to reveal even subtle correlations. This width yields $\sqrt{2} \cdot N$ annuli where N is half the frequency range as discussed above. Hence, at the critical frequency of $\xi_c = N$ the annuli start to exceed the spectral estimate and yield less reliable statistics. This should be marked appropriately.

3.5. *Formatting/Display*

In order to ensure full comparability, we recommend some final touches on the analysis results.

3.5.1. *Tone Mapping*

Spectrum images should conform to a global logarithmic tone mapping. The renderings in this paper were generated using the mapping $x \mapsto \log_2(1 + \alpha x)$ with $\alpha = 0.25$.

3.5.2. *Anisotropy Scale*

When plotting the anisotropy, the axis minimum and maximum value should not exceed the background noise level by more than a factor of ≈ 1.25 for $K \geq 10$. Otherwise, the graph may get significantly compressed, which would suppress potential artifacts.

3.5.3. DC Peak

The DC peak may be removed from all plots because it provides no insight into the spectral characteristics of a specific generation method.

4. Discussion

We tested these parameter settings with a large variety of both deterministic and stochastic point generation methods and they generally worked very well. Although they were designed for the uniform case of nonadaptive point sets in the unit torus, similar recommendations should apply to the nonuniform case using differential domain analysis [Wei and Wang 11]. To support its adoption, we provide an implementation via an open source project at the address listed at the end of this paper.

Acknowledgments. The authors would like to thank Daniel Heck and the anonymous reviewers for their helpful comments and suggestions.

References

- [Dammertz 09] Sabrina Dammertz. “Rank-1 Lattices in Computer Graphics.” Ph.D. thesis, Ulm University, 2009.
- [Lagae and Dutré] Ares Lagae and Philip Dutré. “A Comparison of Methods for Generating Poisson-Disk Distributions.” *Computer Graphics Forum* 27:1 (2008), 114–129.
- [Ostromoukhov 07] Victor Ostromoukhov. “Sampling with Polyominoes.” *Proc. SIGGRAPH '07, ACM Transactions on Graphics* (2007), 78.
- [Proakis and Manolakis 96] John G. Proakis and Dimitris G. Manolakis. *Digital Signal Processing*. New Jersey: Prentice-Hall, 1996.
- [Ulichney 87] Robert Ulichney. *Digital Halftoning*. London, England: MIT Press, 1987.
- [Wei and Wang 11] Li-Yi Wei and Rui Wang. “Differential Domain Analysis for Non-Uniform Sampling.” *Proc. SIGGRAPH '11, ACM Transactions on Graphics* (2011).

Thomas Schlömer, University of Konstanz, Fach 698, D-78457 Konstanz, Germany
(thomas.schloemer@uni-konstanz.de)

Oliver Deussen, University of Konstanz, Fach 698, D-78457 Konstanz, Germany
(oliver.deussen@uni-konstanz.de)